Editors' Suggestion | Featured in Physics

Mapping Twisted Light into and out of a Photonic Chip

Yuan Chen,[1,2,3] Jun Gao,[1,2,3] Zhi-Qiang Jiao,[1,3] Ke Sun,[1] Wei-Guan Shen,[1,3] Lu-Feng Qiao,[1,3] Hao Tang,[1,3,4] Xiao-Feng Lin,[1,3] and Xian-Min Jin[1,3,4,*]

[1]*State Key Laboratory of Advanced Optical Communication Systems and Networks, School of Physics and Astronomy, Shanghai Jiao Tong University, Shanghai 200240, China*

[2]*Institute for Quantum Science and Engineering and Department of Physics, Southern University of Science and Technology, Shenzhen 518055, China*

[3]*Synergetic Innovation Center of Quantum Information and Quantum Physics, University of Science and Technology of China, Hefei, Anhui 230026, China*

[4]*Institute of Natural Sciences, Shanghai Jiao Tong University, Shanghai 200240, China*

(Received 4 May 2018; published 7 December 2018)

Twisted light carrying orbital angular momentum (OAM) provides an additional degree of freedom for modern optics and an emerging resource for both classical and quantum information technologies. Its inherently infinite dimensions can potentially be exploited by using mode multiplexing to enhance data capacity for sustaining the unprecedented growth in big data and internet traffic and can be encoded to build large-scale quantum computing machines in high-dimensional Hilbert space. While the emission of twisted light from the surface of integrated devices to free space has been widely investigated, the transmission and processing inside a photonic chip remain to be addressed. Here, we present the first laser-direct-written waveguide being capable of supporting OAM modes and experimentally demonstrate a faithful mapping of twisted light into and out of a photonic chip. The states OAM_0, OAM_{-1}, OAM_{+1}, and their superpositions can transmit through the photonic chip with a total efficiency up to 60% with minimal crosstalk. In addition, we present the transmission of quantum twisted light states of single photons and measure the output states with single-photon imaging. Our results may add OAM as a new degree of freedom to be transmitted and manipulated in a photonic chip for high-capacity communication and high-dimensional quantum information processing.

DOI: 10.1103/PhysRevLett.121.233602

The phase of an optical beam with a spatial degree of freedom of orbital angular momentum (OAM) is twisted like a corkscrew around its axis of travel and the cancellation of light waves at the axis itself results in a "doughnut" intensity profile. The twisted light has a helical wave front with an azimuthal phase term $e^{i\ell\varphi}$ [1], with which every photon can carry an OAM of $\ell\hbar$ (ℓ is topological charge, φ is azimuthal angle, and $\hbar$ is the Planck constant h divided by 2π). Having the special features of intensity structure (doughnut intensity), phase structure (spiral phase front), and dynamic characteristic (carrying OAM), the twisted light has been widely applied into the field of optical manipulation [2], optical trapping [3,4], and optical tweezers [5].

In recent years, OAM has shown great potential in communication systems for overcoming the channel capacity crunch [6,7]. The unlimited topological charges and the inherent orthogonality may provide tremendous resources for mode multiplexing. The inherently infinite dimensions can also potentially be exploited to deliver high-dimensional quantum states with larger alphabets and to build quantum computing machines in high-dimensional Hilbert space [8–12].

Large-scale applications of OAM beyond proof-of-principle demonstrations require developing integrated devices to enable the generation, transmission, and processing of such a new degree of freedom. Previous works have demonstrated on-chip generation twisted light with integrated star couplers [13], microring resonators [14], and controlled phase arrays [15]. While the emission of twisted light from the surface of integrated devices to free space has been widely investigated, the transmission and processing inside a photonic chip remain to be solved.

In this Letter, we demonstrate a faithful mapping of twisted light into and out of a photonic chip by prototyping doughnut waveguides with femtosecond laser direct writing [16,17]. We couple the states OAM_0, OAM_{-1}, OAM_{+1}, and their superpositions into and out of the photonic chip with a total efficiency up to 60% and verify the output states by interfering with the Gaussian reference beam and making projection measurements, which clearly demonstrate that the output state basically keeps the OAM of the input state. In addition, we present the transmission of single-photon quantum twisted light and measure the output states with single-photon imaging.

 © 2018 American Physical Society

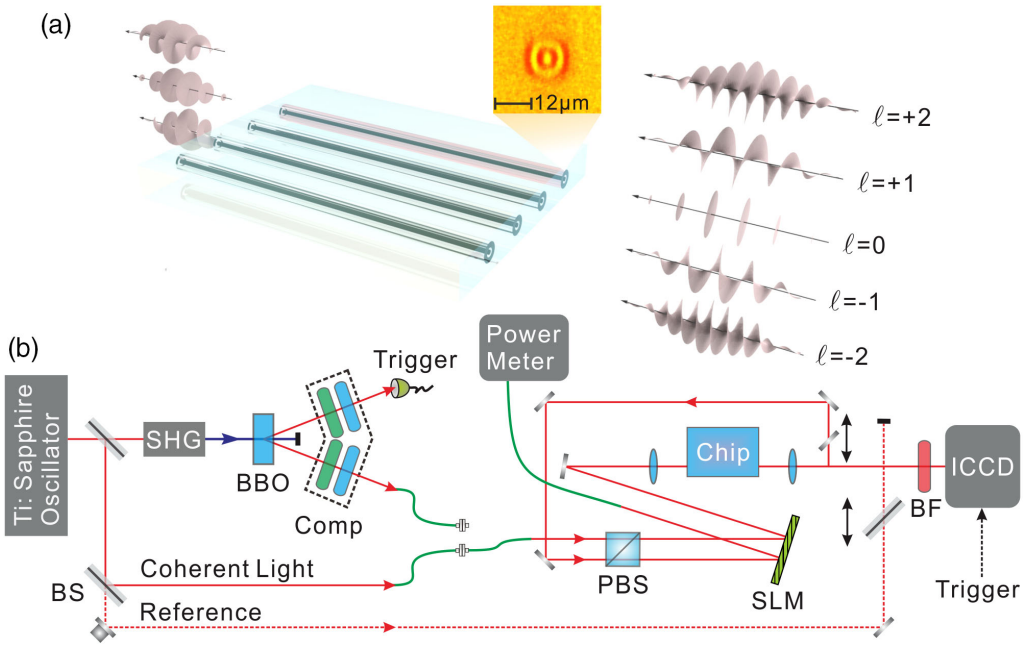

FIG. 1. Experimental implementation. (a) Schematic diagram of mapping twisted light into and out of a photonic chip. The inset shows the cross-section image of a femtosecond laser-written "doughnut" waveguide. The OAM modes are generated externally, then, coupled into the "doughnut" waveguide, and, finally, analyzed after the chip. (b) The experimental setup with classical and quantum probes in OAM degree of freedom. Half of the SLM is used to generate the twisted light, and the other half is used to make a projection measurement for the output states via a standard phase-flattening method. By switching the holograms, we can observe the image in the far field. When the hologram applied to the SLM is opposite to the OAM mode, the far field will be a Gaussian mode, representing an effective projection. We select the Gaussian component and couple the light into a single-mode fiber (green line) to measure the OAM spectra after the transmission by using a power meter. Comp: a half wave plate and a quarter wave plate together are used for polarization compensation; BS: beam splitter; PBS: polarization beam splitter; SLM: spatial light modulator; BF: band-pass filter (780 nm $\pm$ 6 nm); ICCD: intensified charge coupled device camera; BBO: beta-barium borate.

In conventional waveguides, the effective index n_{eff} is much too small to isolate near-degenerate OAM states from one another. A solution to this problem is to enhance the vector splitting through a choice of waveguide structure. It is known that the typical transverse intensity pattern of an OAM beam is doughnut shaped. The waveguides with such a shaped cross section, being cylindrically symmetric in structure, may support OAM modes. The key physical problem of OAM propagating in cylindrically symmetric structures is that, during total internal reflection, phase shifts at index discontinuities critically depend on polarization orientation of an incident wave [18]. To translate this physical problem into a mathematical problem, it can be expressed by a full vectorial solution of the Maxwell equations. By means of a first-order perturbative analysis, it is found that a doughnut waveguide would be more suitable for supporting OAM modes [18].

We realize constructing such a three-dimensional (3D) structure by using a femtosecond laser direct writing technique (see Supplemental Material A [19,20]). The Fig. 1(a) inset shows the cross-section image of the fabricated waveguide, which is measured by an optical microscope with a built-in Kohler illumination system (a halogen lamp light source). We prepare the twisted light in different OAM modes and couple them into the doughnut waveguide embedded in the photonic chip and expect to observe well-preserved output states. After polishing both ends of the chip, the length of the doughnut waveguide is 19.64 mm. As is shown in Fig. 1(b), the probe is switchable to both coherent light and a heralded single photon (see Supplemental Material B [21]). In our experiment, the coupling objective is optimized for mode matching of OAM_{-1}, OAM_{0}, and OAM_{+1} between the free-space beam profile and waveguide cross section. After mapping out the photonic chip, we measure the intensity profile with a CCD camera. The total efficiency is obtained by measuring the probe power before and after the chip, which is up to 60.0%.

The observed intensity profiles of OAM_{-1}, OAM_{0}, and OAM_{+1} modes are shown in Fig. 2(a). The prepared states before mapping into the chip are shown in the first column and the output states are shown in the second column. By inserting a beam splitter, we are able to measure the interference with a Gaussian reference beam. The yielded interference pattern shown in the third column of Fig. 2(a) can be employed to verify the topological charge of the output OAM modes. The high-visibility clockwise (counterclockwise) spiral interference patterns are observed

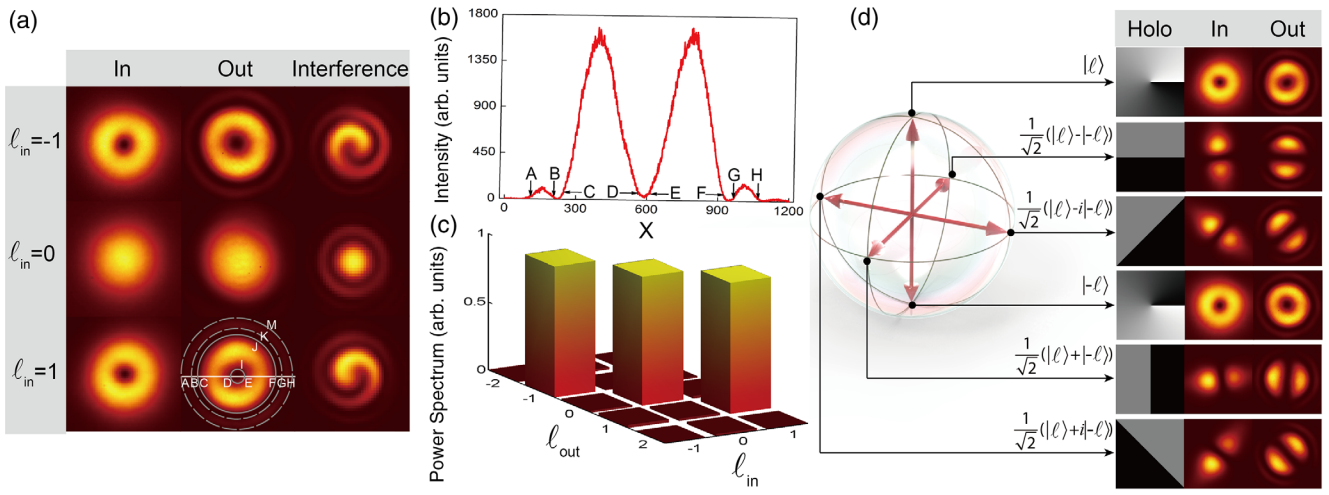

FIG. 2. Experimental results of mapping OAM_{-1}, OAM_0, OAM_{+1}, and their superpositions. (a) The measured intensity profiles of OAM_{-1}, OAM_0, and OAM_{+1} modes before (after) the chip are shown in the first (second) column. Measured interference patterns shown in the third column clearly confirmed faithful preservation of OAM. (b) Radial intensity distribution extracted from the OAM_{+1} mode along the white radial direction. (c) Measured OAM power spectra after the chip. (d) Experimental results of OAM superposition states for $\ell = 1$. The holograms applied to SLM and the measured intensity profiles for six universal states are presented visually pointing to a Bloch sphere.

for the OAM_{+1} (OAM_{-1}) output state, which indicates a great ability to maintain the twisted light.

In order to analyze the output states quantitatively, we take the OAM_{+1} mode after the chip as a typical example for analyzing the intensity ratio between the outer ring and inner ring. *A*, *B*, *G*, and *H* (*C*, *D*, *E*, and *F*) marked in Fig. 2(a) are the junction points of the outer (inner) ring with the white radial direction. By a trapezoidal integration on the 1D radial intensity distribution shown in Fig. 2(b), we multiply it by the ratio of lengths of the two circles (about a factor of 2.5), and, then, we can obtain the power of the outer ring, which is about 7.5% of the inner ring power. More rigorously, we make an integration on the cross area of the rings. We mark the inner (outer) ring with the two solid (dotted) circles *I* and *J* (*K* and *M*). The obtained power of the outer ring is about 6.7% that of the inner ring. This indicates that the radial index has a limited influence on the output state. Therefore, we focus on the azimuth information of OAM modes. As is shown in Fig. 2(c), we make projection measurements (see Supplemental Material C [22]) for the output states and the corresponding percentage of power that remains on the same OAM value after going through the waveguide is over 95.5% on average, which indicates again that the twisted light is well maintained through the chip.

Besides individual pure states, we look further into the ability to support general superposition states. We can construct matrices to describe the superpositions of $OAM_{\pm|\ell|}$ and their transformations on two-dimensional subspaces [23] that can be represented by a Bloch sphere, equivalent to the Poincaré sphere for polarization [24]. By tuning the relative phase and the magnitude of the superposition components on a spatial light modulator, we can access states distributed over the entire Bloch sphere [25]. We show the results of mapping six universal states on a Bloch sphere into and out of the photonic chip, which indicate great capacity to simultaneously support all superposition states [see Fig. 2(d)]. Interestingly, we also observe that output states possess even better spatial structure than the input states. It can be understood that the unwanted components of the imperfect input states can be spatially filtered out by the waveguide that only supports well-defined OAM modes. We attribute the unwanted components generated with the SLM to a convergent Gaussian spot imprinted on it. In addition, an equal-weighted superposition state consisting of OAM_0, OAM_{-1}, and OAM_{+1} can also be transmitted through the chip (see Supplemental Material D [26]), which is a promising hint, that our doughnut-shaped waveguide can support genuinely high-dimensional states in very large spaces.

Our photonic chip is optimized for supporting OAM_0, OAM_{-1}, OAM_{+1}, and their superpositions. It would be interesting to explore the propagation properties of higher-order modes. As is shown in Fig. 3(a), while the sign of positive and negative topological charges are unchanged, the states are all mapped onto their corresponding first-order OAM modes, which are clearly revealed by the chirality and the number of arms in the measured interference patterns.

To understand this, we have also made projection measurements on the input and output states for all the higher-order OAM modes. As is shown in Fig. 3(b), the measured power spectra verifies that the input states for all the higher-order modes are almost pure states with an average purity of up to 94.2%, with a negligible component

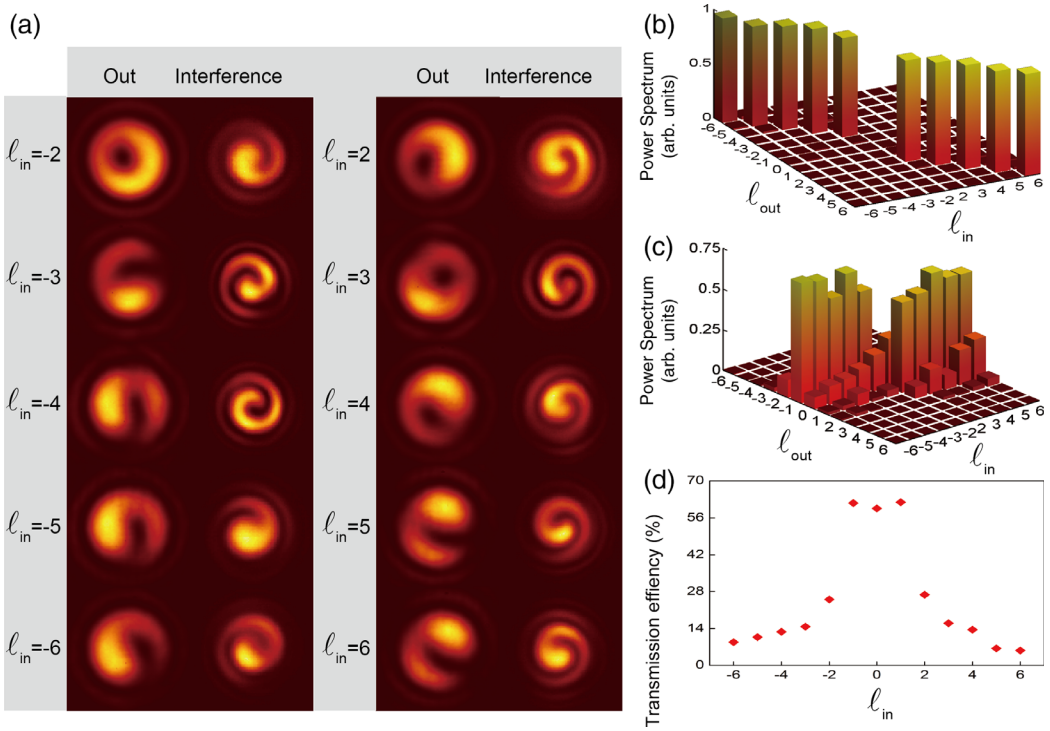

FIG. 3. Experimental mapping of higher-order OAM modes. (a) The measured intensity profiles and interference pattern on the output end of the chip for high order ℓ_{in} up to 6. (b) Measured OAM power spectra before the chip. (c) Corresponding OAM power spectra after the chip. (d) Measured transmission efficiency versus different input states.

of 0.4% (0.5%) for OAM_{+1} (OAM_{-1}). However, the measured power spectra of the output states are found to mainly weigh on the OAM_{-1} or OAM_{+1} mode depending on the chirality of the input states [see Fig. 3(c)]. In particular, for the negative (positive) higher-order input modes, the measured weight of the output states on OAM_{-1} (OAM_{+1}) is dominant, reaching 66.9% (61.2%) on average. These results explain why we can only observe the interference pattern with one spiral arm and chirality.

Further, we measure the transmission efficiency for all the input OAM modes and observe a dramatic drop from the first-order (61.8%) to the second-order (25.9%) input OAM modes [see Fig. 3(d)], while the transmission efficiency drops gradually from the second-order to the sixth-order input OAM modes. Therefore, when a higher-order OAM mode is coupled, it will dissipate and partially evolve into the eigenmode, as the output is always mainly OAM_{-1} (OAM_{+1}). These results imply that the doughnut waveguide has its own eigenmodes OAM_0, OAM_{-1}, and OAM_{+1} (see Supplemental Material E [27,28]) and tends to support the twisted light of lower orders, which further contributes to the observed conversion effect [29].

The inherently infinite dimensions can potentially be exploited as an alternative resource to prepare high-dimensional Hilbert space quantum states, hyperentanglement, for instance, to boost the computational power of quantum computing and quantum simulations rather than to prepare quantum states with a higher photon number. The resource of photonic dimensions seems more scalable than the photon number [30] but requires complex processing circuits and phase-level stability, i.e., is physically unscalable with bulk optics. Quantum integrated photonics would be an elegant solution for such demands. We make the step forward for OAM-based high-dimensional quantum information processing by demonstrating mapping single-photon quantum twisted light into and out of a photonic chip. Thanks to the rapid progress in imaging technologies over the last few years, CCD cameras have become an interesting option for single-photon detection in quantum optics experiments since the large spatial information [31,32] is directly accessible.

In this experiment, we directly visualize quantum twisted light in thermal states and heralded single-photon states before and after the photonic chip by employing an ICCD camera. First, we initialize (or spatially filter) the thermal states and heralded single-photon states with a single-mode fiber before imprinting OAM, which means the photons are all coherent in the transverse spatial domain. The obtained intensity profiles are shown in Fig. 4 without any Fourier-transformation-based noise filtering or background reduction. It should be noticed that the high-quality imaging of heralded single-photon states is achieved because we utilize the detection signal of another photon to trigger the ICCD with a time window as narrow as 10 ns.

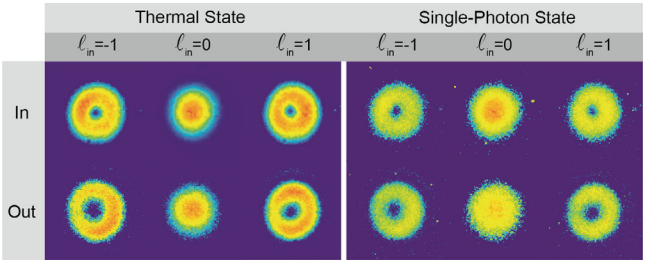

FIG. 4. Experimental results of OAM quantum states. The intensity profiles of quantum twisted light in heralded single-photon states (thermal states) are measured directly with (without) externally triggering the ICCD with another photon. The single-photon images are shown without any reduction of background noises.

In summary, we demonstrate a faithful and highly efficient mapping of twisted light into and out of a photonic chip by prototyping doughnut waveguides with femtosecond laser direct writing. The simultaneous support of the states OAM_{-1}, OAM_0, and OAM_{+1}, and their superpositions suggests that it is possible to transmit and manipulate OAM states inside a photonic chip. We also show the compatibility of single-photon quantum twisted light to the photonic chip and measure the output states with single-photon imaging, which may promise OAM based integrated high-dimensional quantum information processing.

This emerging field of twisted-light-inside integrated photonics has many open problems to be solved. The evanescent light coupling or splitting between two OAM waveguides is a primary goal, which may facilitate the design and fabrication of many novel OAM carrying integrated devices, and, especially, may enable OAM state generation inside a chip by appropriate coupling and phase matching [33]. Quantum interference between the transverse spatial modes has been observed in multimode waveguides [33], which implies that it is possible to realize the first-order or Hong-Ou-Mandel interference for OAM modes inside a photonic chip.

Multichannel all-on-chip senders (receivers) can be conceived to encode (sort) OAM with large alphabet information [34], for both classical and quantum communications. The combined use of different degrees of freedom of a single photon, such as spin and orbital angular momentum, enables the on-chip implementation of entirely new quantum information systems in a high-dimensional space [12,35,36] for quantum supremacy.

The authors thank Miles Padgett, Nathan Langford, and Jian-Wei Pan for helpful discussions and suggestions. This work was supported by the National Key R&D Program of China (Grant No. 2017YFA0303700); National Natural Science Foundation of China (NSFC) (Grants No. 61734005, No. 11761141014, and No. 11690033); Science and Technology Commission of Shanghai Municipality (STCSM) (Grants No. 15QA1402200, No. 16JC1400405, and No. 17JC1400403); Shanghai Municipal Education Commission (SMEC) (Grants No. 16SG09 and No. 2017-01-07-00-02-E00049); X.-M. J. acknowledges support from the National Young 1000 Talents Plan.

*xianmin.jin@sjtu.edu.cn

[1] L. Allen, M. W. Beijersbergen, R. J. C. Spreeuw, and J. P. Woerdman, Orbital angular momentum of light and the transformation of Laguerre-Gaussian laser modes, Phys. Rev. A **45**, 8185 (1992).
[2] K. Dholakia, and T Čižmár, Shaping the future of manipulation, Nat. Photonics **5**, 335 (2011).
[3] L. Paterson, M. P. MacDonald, J. Arlt, W. Sibbett, P. E. Bryant, K. Dholakia, Controlled rotation of optically trapped microscopic particles, Science **292**, 912 (2001).
[4] M. P. MacDonald, L. Paterson, K. Volke-Sepulveda, J. Arlt, W. Sibbett, K. Dholakia, Creation and manipulation of three-dimensional optically trapped structures, Science **296**, 1101 (2002).
[5] M. J. Padgett, and R. Bowman, Tweezers with a twist, Nat. Photonics **5**, 343 (2011).
[6] J. Wang *et al.*, Terabit free-space data transmission employing orbital angular momentum multiplexing, Nat. Photonics **6**, 488 (2012).
[7] N. Bozinovic, Y. Yue, Y. Ren, M. Tur, P. Kristensen, H. Huang, A. E. Willner, and S. Ramachandran, Terabit-scale orbital angular momentum mode division multiplexing in fibers, Science **340**, 1545 (2013).
[8] A. C. Dada, J. Leach, G. S. Buller, M. J. Padgett, and E. Andersson, Experimental high dimensional two-photon entanglement and violations of generalized Bell inequalities, Nat. Phys. **7**, 677 (2011).
[9] R. Fickler, R. Lapkiewicz, W. N. Plick, M. Krenn, C. Schaeff, S. Ramelow, and A. Zeilinger, Quantum entanglement of high angular momenta, Science **338**, 640 (2012).
[10] M. Krenn, M. Huber, R. Fickler, R. Lapkiewicz, S. Ramelow, and A. Zeilinger, Generation and confirmation of a (100×100)-dimensional entangled quantum system, Proc. Natl. Acad. Sci. U.S.A. **111**, 6243 (2014).
[11] M. Mirhosseini, O. S. Magaña-Loaiza, M. N. O'Sullivan, B. Rodenburg, M. Malik, M. P. J. Lavery, M. J. Padgett, D. J. Gauthier, and R. W. Boyd, High-dimensional quantum cryptography with twisted light, New J. Phys. **17**, 033033 (2015).
[12] F. Bouchard, R. Fickler, R. W. Boyd, and E. Karimi, High-dimensional quantum cloning and applications to quantum hacking, Sci. Adv. **3**, e1601915 (2017).
[13] C. R. Doerr *et al.*, Silicon photonic integrated circuit for coupling to a ring-core multimode fiber for space-division multiplexing, in *Proceedings of the European Conference on Optical Communications paper Th.13.A.3, ECOC 2011, Geneva* (Washington, DC, Optical Society of America, 2011).
[14] X.-L. Cai, J. Wang, M. J. Strain, B. Johnson-Morris, J. Zhu, M. Sorel, J. L. O'Brien, M. G. Thompson, and S. Yu, Integrated compact optical vortex beam emitters, Science **338**, 363 (2012).

[15] J. Sun, M. Moresco, G. Leake, D. Coolbaugh, and M. R. Watts, Generating and identifying optical orbital angular momentum with silicon photonic circuits, Opt. Lett. **39**, 5977 (2014).
[16] R. G. Rafael, and E. Mazur, Femtosecond laser micromachining in transparent materials, Nat. Photonics **2**, 219 (2008).
[17] A. Szameit, and S. Nolte, Discrete optics in femtosecond-laser-written photonic structures, J. Phys. B **43**, 163001 (2010).
[18] S. Ramachandran and P. Kristensen, Optical vortices in fiber, Nanophotonics **2**, 455 (2013).
[19] See Supplemental Material A at http://link.aps.org/supplemental/10.1103/PhysRevLett.121.233602 for 3D fabrication of doughnut waveguides, which includes Ref. [20].
[20] R. Osellame *et al.*, *Femtosecond Laser Micromachining: Photonic and Microfluidic Devices in Transparent Materials* (Springer, New York, 2012).
[21] See Supplemental Material B at http://link.aps.org/supplemental/10.1103/PhysRevLett.121.233602 for experiment details about classical and quantum twisted light preparation.
[22] See Supplemental Material C at http://link.aps.org/supplemental/10.1103/PhysRevLett.121.233602 for the detailed power spectrum measurement.
[23] L. Allen, J. Courtial, and M. J. Padgett, Matrix formulation for the propagation of light beams with orbital and spin angular momenta, Phys. Rev. E **60**, 7497 (1999).
[24] M. J. Padgett, and J. Courtial, Poincaré-sphere equivalent for light beams containing orbital angular momentum, Opt. Lett. **24**, 430 (1999).
[25] B. Jack, A. M. Yao, J. Leach, J. Romero, S. Franke-Arnold, D. G. Ireland, S. M. Barnett, and M. J. Padgett, Entanglement of arbitrary superpositions of modes within two-dimensional orbital angular momentum state spaces, Phys. Rev. A **81**, 043844 (2010).
[26] See Supplemental Material D at http://link.aps.org/supplemental/10.1103/PhysRevLett.121.233602 for high-dimensional superposition state.
[27] See Supplemental Material E at http://link.aps.org/supplemental/10.1103/PhysRevLett.121.233602 for additional data about the effect of different coupling systems on the higher-order results, which includes Ref. [28].
[28] J. E. Curtis and D. G. Grier, Structure of Optical Vortices, Phys. Rev. Lett. **90**, 133901 (2003).
[29] Y. Yang, G. Thirunavukkarasu, M. Babiker, and J. Yuan, Orbital-Angular-Momentum Mode Selection by Rotationally Symmetric Superposition of Chiral States with Application to Electron Vortex Beams, Phys. Rev. Lett. **119**, 094802 (2017).
[30] R. Fickler, G. Campbell, B. Buchler, P. K. Lam, and A. Zeilinger, Quantum entanglement of angular momentum states with quantum numbers up to 10,010, Proc. Natl. Acad. Sci. U.S.A. **113**, 13642 (2016).
[31] R. Fickler, M. Krenn, R. Lapkiewicz, S. Ramelow, and A. Zeilinger, Real-time imaging of quantum entanglement, Sci. Rep. **3**, 1914 (2013).
[32] D.-S. Ding, Z.-Y. Zhou, B.-S. Shi, and G.-C. Guo, Single-photon-level quantum image memory based on cold atomic ensembles, Nat. Commun. **4**, 2527 (2013).
[33] A. Mohanty, M. Zhang, A. Dutt, S. Ramelow, P. Nussenzveig, and M. Lipson, Quantum interference between transverse spatial waveguide modes, Nat. Commun. **8**, 14010 (2017).
[34] H. Bechmann-Pasquinucci and W. Tittel, Quantum cryptography using larger alphabets, Phys. Rev. A **61**, 062308 (2000).
[35] M. Krenn, M. Malik, M. Erhard, and A. Zeilinger, Orbital angular momentum of photons and the entanglement of Laguerre-Gaussian modes, Phil. Trans. R. Soc. A **375**, 20150442 (2017).
[36] M. Erhard, R. Fickler, M. Krenn, and A. Zeilinger, Twisted photons: New quantum perspectives in high dimensions, Light Sci. Appl. **7**, 17146 (2018).